

# A polychromator-type near-infrared spectrometer with a high-sensitivity and high-resolution photodiode array detector for pharmaceutical process monitoring on the millisecond time scale

著者	Murayama Kodai, Genkawa Takuma, Ishikawa Daitaro, Komiyama Makoto, Ozaki Yukihiro
雑誌名	Review of scientific instruments
巻	84
号	2
ページ	023104
発行年	2013-02
権利	(C) 2013 American Institute of Physics This article may be downloaded for personal use only. Any other use requires prior permission of the author and the American Institute of Physics. The following article appeared in Rev. Sci. Instrum. 84, 023104 (2013) and may be found at <a href="http://link.aip.org/link/?rsi/84/023104">http://link.aip.org/link/?rsi/84/023104</a>
URL	<a href="http://hdl.handle.net/2241/119238">http://hdl.handle.net/2241/119238</a>

doi: 10.1063/1.4790413

## A polychromator-type near-infrared spectrometer with a high-sensitivity and high-resolution photodiode array detector for pharmaceutical process monitoring on the millisecond time scale

Kodai Murayama, Takuma Genkawa, Daitaro Ishikawa, Makoto Komiyama, and Yukihiro Ozaki

Citation: *Rev. Sci. Instrum.* **84**, 023104 (2013); doi: 10.1063/1.4790413

View online: <http://dx.doi.org/10.1063/1.4790413>

View Table of Contents: <http://rsi.aip.org/resource/1/RSINAK/v84/i2>

Published by the [American Institute of Physics](#).

---

### Additional information on *Rev. Sci. Instrum.*

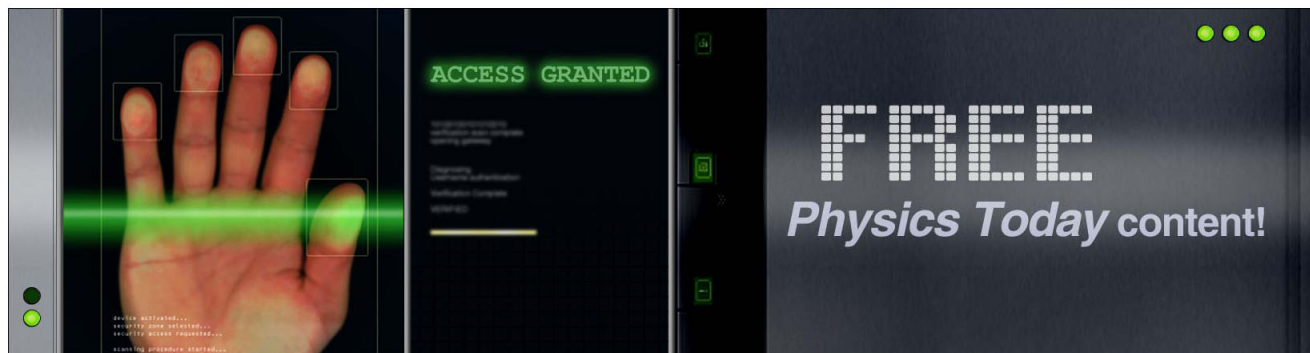
Journal Homepage: <http://rsi.aip.org>

Journal Information: [http://rsi.aip.org/about/about\\_the\\_journal](http://rsi.aip.org/about/about_the_journal)

Top downloads: [http://rsi.aip.org/features/most\\_downloaded](http://rsi.aip.org/features/most_downloaded)

Information for Authors: <http://rsi.aip.org/authors>

## ADVERTISEMENT



# A polychromator-type near-infrared spectrometer with a high-sensitivity and high-resolution photodiode array detector for pharmaceutical process monitoring on the millisecond time scale

Kodai Murayama,<sup>1</sup> Takuma Genkawa,<sup>2,3</sup> Daitaro Ishikawa,<sup>2</sup> Makoto Komiyama,<sup>1,a)</sup> and Yukihiro Ozaki<sup>2,a)</sup>

<sup>1</sup>*Sensing Technology Research Center, Innovation Headquarters, Yokogawa Electric Corporation, 2-9-32 Nakacho, Musashino 180-8750, Japan*

<sup>2</sup>*Department of Chemistry, School of Science and Technology, Kwansei Gakuin University, 2-1 Gakuen, Sanda 669-1337, Japan*

<sup>3</sup>*Faculty of Life and Environmental Sciences, University of Tsukuba, 1-1-1 Tennodai, Tsukuba 305-8572, Japan*

(Received 14 November 2012; accepted 22 January 2013; published online 13 February 2013)

In the fine chemicals industry, particularly in the pharmaceutical industry, advanced sensing technologies have recently begun being incorporated into the process line in order to improve safety and quality in accordance with process analytical technology. For estimating the quality of powders without preparation during drug formulation, near-infrared (NIR) spectroscopy has been considered the most promising sensing approach. In this study, we have developed a compact polychromator-type NIR spectrometer equipped with a photodiode (PD) array detector. This detector is consisting of 640 InGaAs-PD elements with 20- $\mu$ m pitch. Some high-specification spectrometers, which use InGaAs-PD with 512 elements, have a wavelength resolution of about 1.56 nm when covering 900–1700 nm range. On the other hand, the newly developed detector, having the PD with one of the world's highest density, enables wavelength resolution of below 1.25 nm. Moreover, thanks to the combination with a highly integrated charge amplifier array circuit, measurement speed of the detector is higher by two orders than that of existing PD array detectors. The developed spectrometer is small (120 mm  $\times$  220 mm  $\times$  200 mm) and light (6 kg), and it contains various key devices including the high-density and high-sensitivity PD array detector, NIR technology, and spectroscopy technology for a spectroscopic analyzer that has the required detection mechanism and high sensitivity for powder measurement, as well as a high-speed measuring function for blenders. Moreover, we have evaluated the characteristics of the developed NIR spectrometer, and the measurement of powder samples confirmed that it has high functionality. © 2013 American Institute of Physics. [<http://dx.doi.org/10.1063/1.4790413>]

## I. INTRODUCTION

In the pharmaceutical industry, at a worldwide level, the development and approval of new drugs is increasingly being governed by common regulations. In this scenario, there has emerged the need for a quality assurance method with a strong scientific basis. To satisfy this need, the U.S. Food and Drug Administration proposed process analytical technology (PAT) for the design, analysis, and control of pharmaceutical manufacturing processes through the timely measurement of the critical process parameters that affect the final product quality. This technique is expected to replace conventional validation techniques and realize improved manufacturing efficiency and quality control of pharmaceuticals.<sup>1–4</sup>

PAT is used to analyze the manufacturing process, determine the factors essential for understanding the manufacturing process, and clarify variable factors that affect quality control. At the same time, it is important to improve the manufacturing process based on the results of PAT. From these viewpoint, real-time measurement is essential. Toward

this end, spectroscopy, in particular, near-infrared (NIR) spectroscopy, has attracted considerable interest because it affords several advantages such as noncontact and nondestructive measurements and availability of remote detection by optical fiber.<sup>5–10</sup>

The Fourier transform method is widely used in NIR spectrometers; this method obtains the spectrum by the Fourier transform of interference signal data acquired while changing the optical path length.<sup>7</sup> It needs a wavelength standard, and therefore, it has very high wavelength accuracy. Moreover, in principle, it has superior optical throughput. Finally, various improvements have recently been made to the drive mechanism of the variable optical length, data processing, and so on. The monochromator-type spectroscopic method is also widely used in NIR spectrometers; this method is a wavelength dispersion method.<sup>8</sup> In this method, the wavelength is continuously swept by changing the angle of the diffraction grating. The advantages of this method are the high dynamic range and high wavelength resolution. However, it does have some disadvantages, such as the long measurement time, large size, and lack of robustness owing to the wavelength being swept mechanically. The laser-scanning-type method is used to sweep the emission wavelength by

<sup>a)</sup>Authors to whom correspondence should be addressed. Electronic addresses: Makoto.Komiyama@jp.yokogawa.com and ozaki@kwansei.ac.jp.

varying the current or the external cavity. Although the measurement wavelength area is limited to the range of laser emission, this method has advantageous features such as high dynamic range and high wavelength resolution. In this method, multiple lasers with different emission wavelength regions are required to cover the measured NIR wavelength region. The method, which uses a polychromator, employs a spatial wavelength dispersion device, and it enables detection over a wavelength region by using a multichannel detector. Unlike in the monochromator-type method, this method simultaneously detects multiple beams over a wavelength region. The number of channels in the multichannel detector determines the wavelength resolution. This method has advantageous features such as high-speed measurement, robustness, and compactness owing to the non-mechanical moving architecture.<sup>9</sup>

These methods involve specific advantages and disadvantages, and it is necessary to select one that is most suitable for use as an in-line analyzer. Generally speaking, this PAT application requires features such as high-speed measurement, compact size, and maintainability (if possible, maintenance-free). The polychromator-type method provides these features; however, its wavelength resolution is inferior to that of other methods. If the wavelength resolution of this method could be improved, it would become the best method for in-line spectroscopy. To improve the wavelength resolution of this method, it is necessary to increase the pixel number of the photodiode array (PDA);<sup>10</sup> the pixel number of PDA also determines the PDA device size. The spectrometer size increases in proportional to the PDA device size. In other words, both wavelength resolution improvement and device miniaturization can be achieved by increasing the pixel number and density of PDA.

In the present study, we have developed a new PDA detector that combines a high-density array with a charge-amplifier-array-type integrated circuit (IC). It holds PDA with one of the world's highest density (20- $\mu\text{m}$  pitch) and unusual high speed (<10 ms). This novel detector has allowed us to improve the wavelength resolution and detection sensitivity of the polychromator-type NIR spectrometer (P-NIRs). We have designed a new P-NIRs using this PDA as well as an improved optical probe to improve the sensitivity. The wavelength resolution and sensitivity of the P-NIRs were evaluated through the measurement of a powder sample, and its applicability to an in-line monitoring process was examined through the measurement of a powder mixture process.

## II. DEVELOPMENT OF HIGH-DENSITY AND HIGH-SENSITIVITY PDA DETECTOR

### A. High-density PDA

The detector consists of a high-density PDA containing 640 elements with 20- $\mu\text{m}$  pitch. InGaAs photodiodes with a wavelength sensitivity of 900–1700 nm (photoreceptive sensitivity: 0.8 at 1550 nm) are used. The wavelength resolution of the NIR spectrometer, which uses the new PDA with 640 elements, is 60% higher than that of a conventional high-specification NIR spectrometer that has a PDA with 256 elements. If a measurement wavelength region is 900–1700 nm,

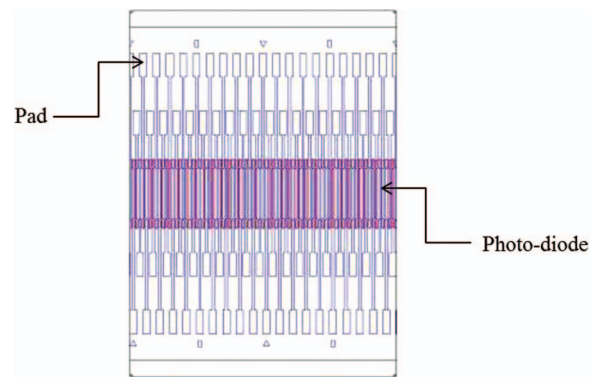


FIG. 1. Part of the 640-element PDA.

the wavelength resolution is 3.1 nm for a spectrometer with a PDA having 256 elements while it is 1.25 nm for that with the 640 elements. Figure 1 shows a diagram of a part of the newly developed PDA. This is a PN-junction-type PDA. The substrate structure of the photodiode is formed by growing an InGaAs optical absorption layer on an InP-based substrate by epitaxial growth and then growing an InP cap layer on the InGaAs optical absorption layer. Moreover, an InP buffer layer is formed between the InP substrate and the InGaAs photoabsorption layer. A SiO<sub>2</sub> mask pattern is formed in order to form the 640-element PDA with 20- $\mu\text{m}$  pitch and 10- $\mu\text{m}$  photoreceptive width on the substrate. Zn is diffused into the obtained substrate to form a high-density PN-junction-type PDA. The PDA converts the energy of incident light into a photocurrent. The PDA may suffer from fluctuations in the current output owing to light energy entering between two adjacent PDs. To prevent these fluctuations and to improve sensitivity, an optical cover material was placed between adjacent PDs.<sup>11–13</sup> Figure 1 shows a chart of the electrode pattern of the PDA. The 640 elements in the PDA are divided into two sets of 320 elements based on whether the pixel number is even or odd. Moreover, the bonding pads are arranged in a staggered manner with a two-step arrangement. In this manner, the array density could be increased.

### B. Charge amplifier array silicon integrated circuit

A charge-amplifier-array-type Si-IC that amplifies the photocurrent converted by the 640-element PDA was also newly developed. Figure 2 shows a block diagram of the charge-amplifier-array-type Si-IC. It consists of a 320-element charge amplifier array that is highly integrated to match with a PDA with world top class density, a sample hold circuit, a shift register circuit, and a timing generator circuit. A photocurrent from the photodiodes charges the integral capacitor, and the electric charge is converted into a voltage by the charge amplifier. The output voltage can be calculated by Eq. (1)

$$V_s = \frac{(I_s + I_d) T_c}{C_f}, \quad (1)$$

where  $V_s$  [V],  $I_s$  [A],  $I_d$  [A],  $T_c$  [s], and  $C_f$  [F] indicate the output voltage, signal current, dark current, charge time, and integral capacitance, respectively.



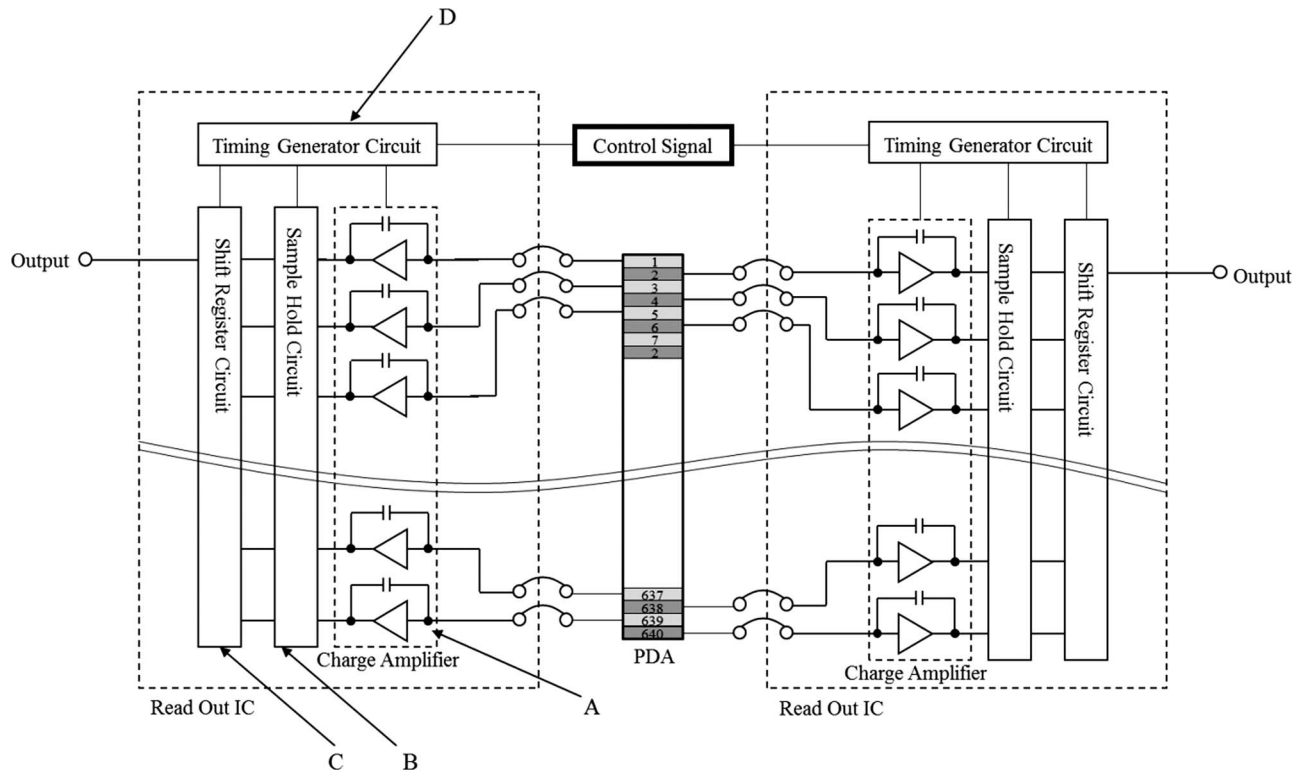


FIG. 2. Block diagram of PDA: (A) 320-element charge amplifier array, (B) sample hold circuit, (C) shift register circuit, and (D) timing generator circuit. Two ROICs and one PDA are assembled by the wire bonding method.

The charge amplifier can maintain a high dynamic range by having, and selecting two integral capacitors (that have values of 0.5 and 10.). All elements of the charge amplifier array work completely at the same time by the clock synchronous method that is controlled by the timing generator circuit. The charge time is controlled based on the external input pulse width. The signal of each element after charging was completed is held by the sample hold circuit, following which each signal is read one-by-one by the shift register circuit at high speed. The bonding pad arrangement of the charge-amplifier-array type Si-IC is the same as that of the PDA.

Existing PDAs individually acquire the photocurrent signal converted by each element by using an external amplifier, and therefore, they require a measurement time of sub-seconds to detect the signal level. In contrast, the newly developed PDA acquires the photocurrent signal converted by each element simultaneously using the charge-amplifier-array-type Si-IC, and therefore, it requires a measurement time of less than 10 ms.

### C. Photodiode array detector

Figure 3 shows the newly developed photodiode array sensor. An AlN substrate was selected owing to its good heat conduction and other features. At its center, it contains 640 InGaAs photodiode elements with 20- $\mu\text{m}$  pitch, which we believe to be the highest density reported thus far in the world, on both sides of the substrate, and the newly developed charge-amplifier-array-type Si-IC is mounted on top of this. The substrate is mounted on a ceramic package via a

thermoelectric cooler and is sealed with a cap with a sapphire window after filling with  $\text{N}_2$ .

To evaluate the sensitivity and speed of the PDA, the noise characteristics were evaluated. The light receiving surface was shaded, and 100 measurements were carried out with an operation temperature of 25  $^{\circ}\text{C}$ , charge time of 10 ms, and integral capacitance of 0.5 pF. The root mean square noise voltage ( $V_{rms}$ ) of each pixel was calculated from the measured data, and the root mean square noise current ( $I_{rms}$ ) of each pixel was calculated by Eq. (1). Figure 4 shows a plot of the root mean square noise current of each pixel. The root mean square noise current of each pixel in the PDA was less than 0.03 pA. Moreover, the noise equivalent power (NEP) was calculated by Eq. (2)

$$\text{NEP} = \frac{I_{rms}}{S}, \quad (2)$$

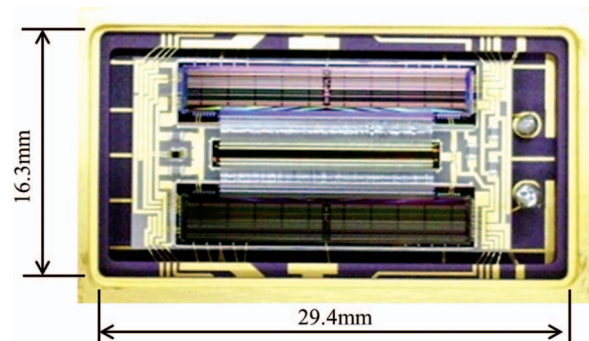


FIG. 3. Outline view of photodiode array sensor.

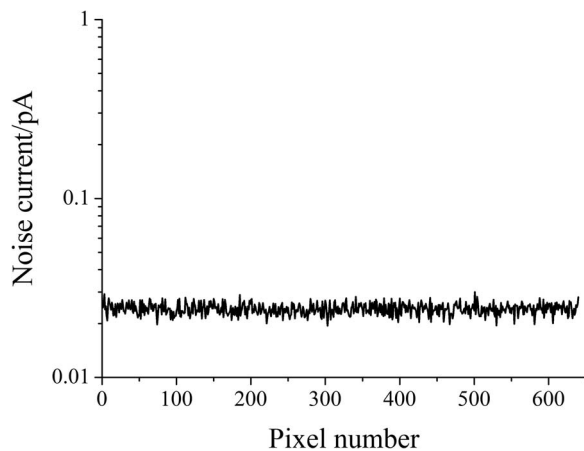


FIG. 4. Plot of root mean square noise current of each pixel.

where the photoreceptive sensitivity is 0.8 A/W at 1550 nm. In all pixels, NEP was less than 0.0375 pW, demonstrating that the newly developed PDA can detect even a feeble light.

### III. DESIGN OF NIR SPECTROMETER

#### A. Development of polychromator-type NIR spectrometer

In the present study, we developed two types of P-NIRs: one with an optical fiber interface (FIF) model with a diffuse reflectance (DR) optical fiber probe for remote measurement, and one with a direct interface (DIF) model with a built-in DR optical fiber probe. Figures 5 and 6 show the FIF and DIF, respectively. Both P-NIRs consists of a polychromator equipped with a PDA detector, an internal optical source (halogen lamp, 5 W), an 18-bit analog to digital (AD) convertor for signal conversion and CPU, a data interface, a power supply (battery and external source), and a DR optical fiber probe. The optical fiber for irradiating light is connected with a built-in optical source, and the optical fiber for receiving light diffuse-reflected from a sample is connected with the spectrometer. Figure 7 shows a schematic diagram of the P-NIRs spectroscopy system, and Table I summarises the specifications

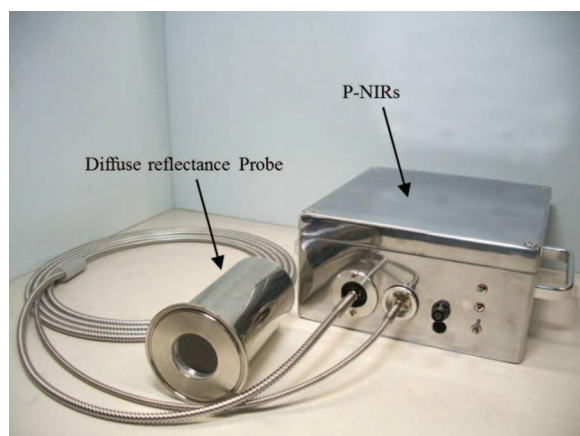


FIG. 5. Fiber interface model of P-NIRs equipped with diffuse reflectance probe.

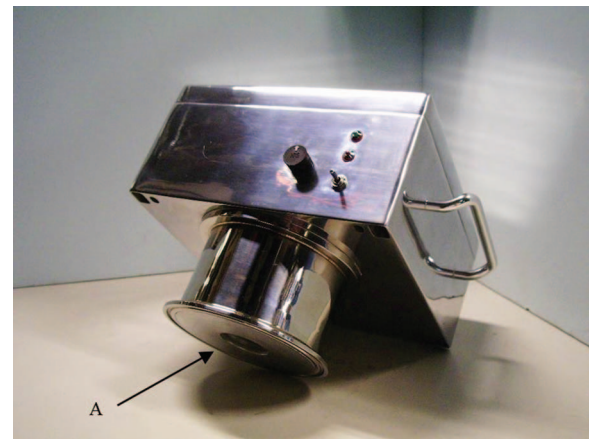


FIG. 6. Direct interface model of P-NIRs. (A) Optical window through which the irradiating and the diffuse reflected light are transmitted.

of this system. A halogen lamp is used to irradiate the samples with NIR light through the optical fiber. The optical fiber comprises a bundle of approximately 100 optical fibers with a core diameter of 190  $\mu\text{m}$ . The DR light enters the spectrometer through the optical fiber, and it is dispersed by the wavelength dispersion device. The dispersed light is irradiated on the PDA by a condensing lens. The PDA output is converted by the 18-bit AD converter and the CPU carries out calculation processes such as the averaging on it. Thereafter, the data sent to a control computer as spectrum data.

The targeted measurement performance of the P-NIRs is inspection of the process line in 10 ms. Toward this end, the P-NIRs employs a high-speed AD converter ( $1 \times 10^6$  samples/s), a digital signal processor, and parallel processing of data. Separately, the P-NIRs has functions such as the wireless data interface, battery operation, and external synchronous sampling of data. The P-NIRs is controlled by a control computer through a serial or a wireless communication protocol. The P-NIRs receives instructions (control commands) from the control computer, and executes the spectral measurement, process data, and transfer data. The absorption spectrum is displayed and saved on the control computer.

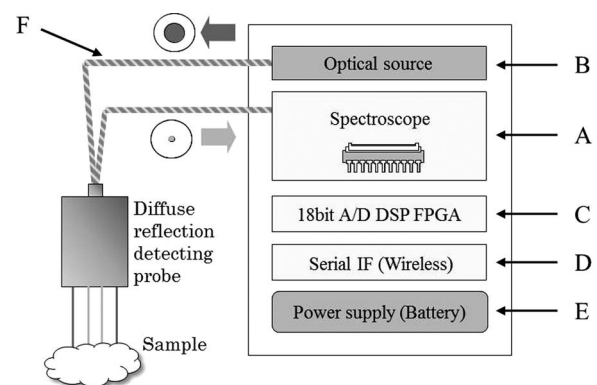


FIG. 7. Spectroscopic analyzer configuration: (A) spectroscopy with a PDA detector, (B) internal optical source, (C) 18-bit analog/digital convertor for signal conversion and CPU, (D) data interface, (E) power supply (battery and external source), and (F) optical fiber probe.

TABLE I. Specification of P-NIRs.

Item	Fiber-interface model	Direct-interface model
Spectral range		900–1700 nm
Wavelength resolution		< 1.25 nm
Wavelength accuracy		< 0.1 nm
Absorbance noise level		< 0.1 mAbs.
Sampling time		Min. 1 ms/spectrum
Measurement interval		Min. 10 ms
Number of PD elements		640 elements
Optical interface	Optical fiber input	Direct: through an optical window
	Serial communication: RS232C, USB	
	Wireless LAN: 802.11b	
Size	120 mm × 220 mm × 200 mm	160 mm × 220 mm × 200 mm
Weight	< 6 kg	< 7 kg
Power supply		ac/dc, battery typ. 15 W
Operating temperature		+5 to 45 °C
Operating humidity		5%–90% RH

## B. Spectro-engine of P-NIRs

Figure 8 shows the spectro-engine of P-NIRs. The light diffuse reflected from a sample is collimated by the collimator lens, and collimated light enters the diffraction grating. The light is diffracted into beams of each wavelength. The light is focused onto the pixels of the PDA by using a focusing lens in conjunction with a mirror. The intensity of the beams of each wavelength is detected by the PDA, and the spectral data are obtained through signal processing.

## C. Diffuse reflectance optical fiber probe for high sensitivity

In the present study, a DR optical fiber probe was also newly developed for convenient and sensitive spectral measurement. This optical fiber probe consists of the condensing lens and the optical fiber bundle. The lens condenses the irradiating light and the light diffuse-reflected from the sample. By changing the focusing distance of the condensing lens, one can flexibly vary the working distance between the probe and

the sample. The optical fiber bundle is an assembly of optical fibers that transmits the irradiating and diffuse reflection lights. The optical fiber bundle is bunched together at one end, and it is separated into the optical fibers for the irradiating light and the optical fiber for the diffuse reflection light at the other end.

The irradiating light intensity increases as the caliber of optical fiber increases, and the detection property improves, on one hand, it also leads to an increase in the mechanical fragility. The optical fiber bundle was selected and the composition was examined, to achieve a certain mechanical strength, a sufficient light intensity, and a high optical wavelength resolution. We found that one of the best solution to achieve this is the combination of the multimode fiber for detection and a large number of high numerical aperture, small diameter, optical fibers for irradiation. About 100 optical fibers of its guiding diameter of 200  $\mu\text{m}$  allowed us to realize a certain mechanical strength, adequate diameter, and a high efficiency.

We developed a DIF model spectrometer that has a built-in DR probe shown in Fig. 6, for the direct installation to a rotation blender. The DIF model has a three-axis accelerometer to detect its posture, wireless data interface, and lithium ion batteries.

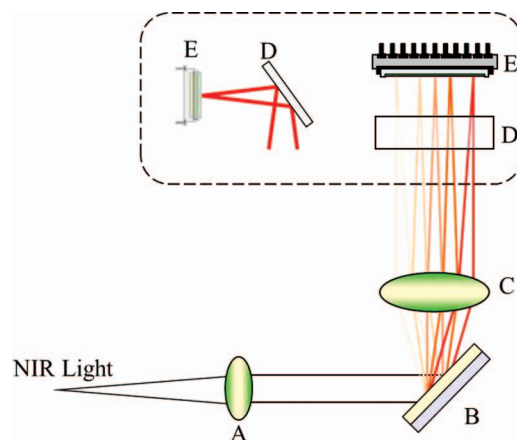


FIG. 8. Spectro-engine of P-NIRs: (A) collimator lens, (B) diffraction grating, (C) focusing lens, (D) mirror, and (E) 640-element PDA.

## IV. EXPERIMENTAL

### A. Evaluation of wavelength resolution

To demonstrate importance of the wavelength resolution and detection sensitivity of P-NIRs, we measured the DR-NIR spectra of talc ( $\text{Mg}_3\text{Si}_4\text{O}_{10}(\text{OH})_2$ , Kanto Chemical Co., Inc.) by using the DR optical fiber probe (FIF model). The distance between the probe and the talc powder was approximately 50 mm, the sampling time was 30 ms, and averaged spectrum calculated from 10 spectra was obtained; the total acquisition time for one spectrum was 0.3 s. Moreover, a halogen lamp (5 W) was used as the light source.

The NIR spectra generally have two major drawbacks: band overlaps are severe and the baseline fluctuation of

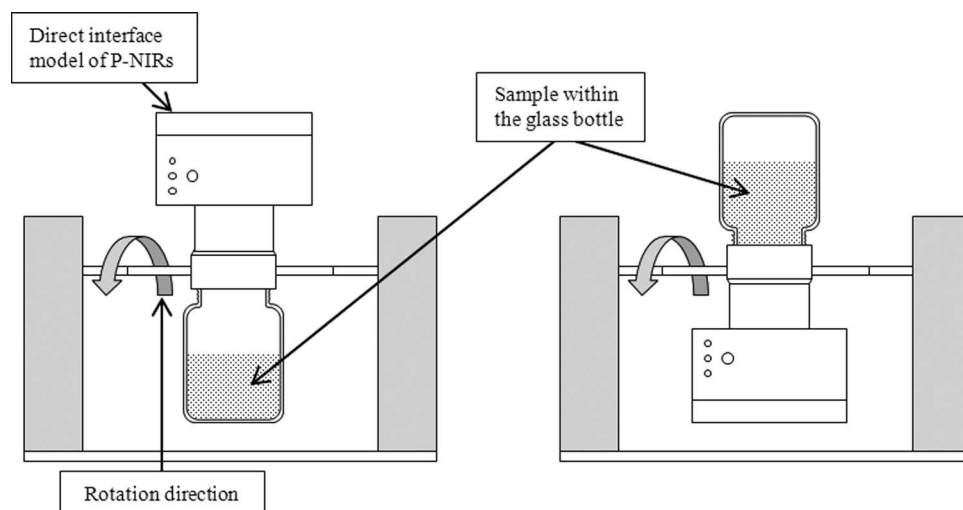


FIG. 9. Blending test setup.

the spectra is often considerable. The second-derivative pretreatment of the spectra is essential for overcoming these problems. If the wavelength resolution of an obtained NIR spectrum is low, it is difficult to separate overlapping bands because the spectrum is distorted. Therefore, the band separation result by the second-derivative pretreatment is also affected by the wavelength resolution. Thus, we have assumed that one can evaluate the wavelength resolution by calculating the second derivative of the spectrum.

To evaluate the wavelength resolution of P-NIRs that of the NIR spectrum obtained with a 1-nm wavelength resolution was decreased to 5 and 10 nm by the simple moving average method. These spectra were subjected to the second-derivative treatment by the Savitzky-Golay method (smoothing point: 11 point).<sup>14</sup>

## B. Blending monitoring test

To evaluate the high-speed performance of P-NIRs, we measured the dynamic mixture spectra of talc and D-mannitol ( $\text{HOCH}_2(\text{CHOH})_4\text{CH}_2\text{OH}$ , Kanto Chemical Co., Inc.) during rotation mixing with the DIF model of P-NIRs. Monitoring powder blending process by using NIR spectroscopy has been investigated,<sup>15–17</sup> because it is highly desired to detect the homogeneity of mixed powder. The outline of the blending test setup is shown in Fig. 9. When DR method is used to measure a spectrum, it is highly desirable to keep an irradiation distance constant, however, powder under mixing always moves and the irradiation distance changes largely during spectral measurement. Therefore, high speed is highly requested for the NIR spectral measurement in blending process.

The 2-l glass bottle is connected with the clump ferrule of the DIF model of P-NIRs. The center of rotation is in the connected part, and the rotation speed is 12 rpm. First, a 300 g of talc was put into the glass bottle, and then, a 700 g of D-mannitol was added on the talc sample. When P-NIRs is in the bottom position the mixture sample in the bottle reaches

the optical window (sapphire), so this timing is adopted as a measurement point. The spectral measurement is performed by detecting the measuring points by the built-in three-axis accelerometer during rotation. The sampling time was 30 ms, and averaged spectrum calculated from 30 spectra was obtained; the total acquisition time for one spectrum was 0.9 s. The light source is a halogen lamp of only 5 W.

## V. RESULTS AND DISCUSSION

### A. Change in spectral shape in the second-derivative spectra with difference in wavelength resolution

Figure 10 shows the second-derivative spectra of talc with wavelength resolution of 1, 5, and 10 nm. It yields a sharp peak at 1392 nm owing to the first overtone stretching mode of the OH group.<sup>18</sup> The second-derivative spectrum with 1-nm wavelength resolution measured by P-NIRs shows a narrow band shape, but the second-derivative spectrum with 5-nm and 10-nm wavelength resolution show a broad band shape. Moreover, in the second-derivative spectrum with 10-nm wavelength resolution, the peak intensity decreased to one half of that of obtained with 1-nm wave-

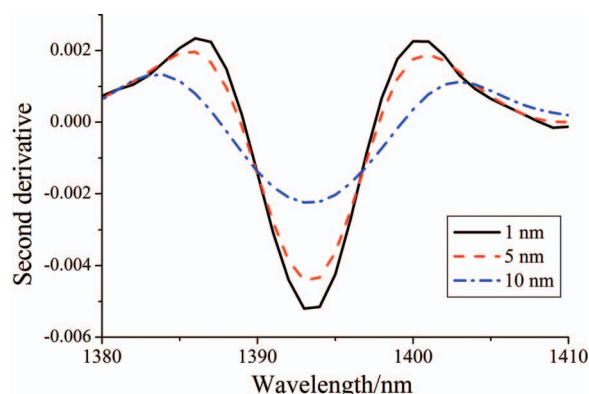


FIG. 10. Second-derivative spectra of talc with different wavelength resolutions.



length resolution. It has been found that the low wavelength resolution exerts a large influence on the band separation performance. Thus, it has been confirmed that high wavelength resolution is very effective for the band separation in certain application. And, it has been shown that the wavelength resolution of the newly developed P-NIRs is sufficiently high. In general, NIR spectral measurements do not require as high a spectral resolution as that required by IR and Raman spectral measurements. However, in the case of pharmaceutical applications high wavelength resolution is needed because pharmaceutical industry requests high precision analysis and high precision discrimination of raw materials. Moreover, DR method often needs a pretreatment such as second derivative, where wavelength resolution controls analysis performance as shown in Fig. 10. Therefore, NIR spectrometers for PAT should have high wavelength resolution, and P-NIRs is equipped with a high wavelength resolution required for PAT application.

### B. Blending process monitoring test of the modeling tablet

Figure 11 shows some DR-NIR spectra of the D-mannitol and talc mixture, measured during rotation mixing. Because of high speed of P-NIRs, we could obtain spectral data at each rotation. The spectrum at 0 s reflects D-mannitol only, and the bands at 1495 and 1580 nm are owing to the first overtones of the OH and CH stretching vibration modes. As spectral variations during rotation mixing, both the change in spectral shape and the baseline fluctuation were observed. In general, baseline fluctuation in DR-NIR spectra during powder mixing is mainly caused by the variance of irradiation distance, but the blending monitor by P-NIRs with position sensor could keep the irradiation distance constant. Therefore, it is considered that the baseline fluctuation reflects change in the mean particle size of mixture powder at the irradiated area.

Figure 12 shows the second derivative of the spectra shown in Figure 11. These spectra were subjected to the second-derivative treatment by the Savitzky-Golay method (smoothing point: 31 point). In the original spectra baseline changed largely, while in the second-derivative spectra we

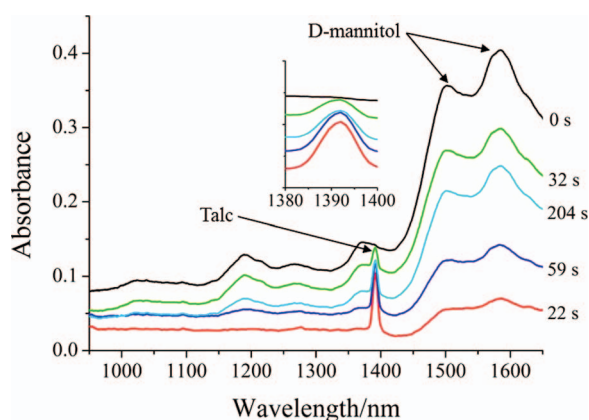


FIG. 11. DR-NIR spectra of the D-mannitol and talc during mixing.

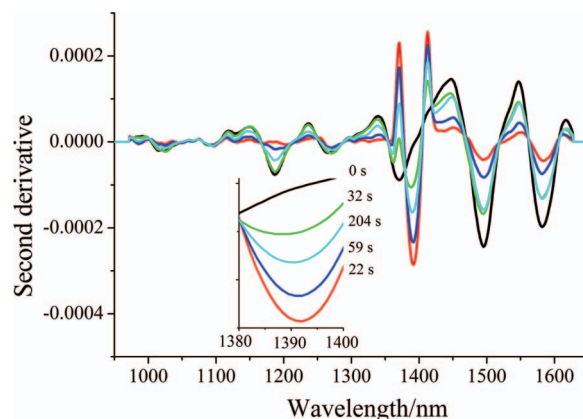


FIG. 12. Second-derivative spectra of the D-mannitol and talc during mixing.

could observe relative intensity changes between the band at 1392 nm due to talc and those at 1495, 1580 nm arising from D-mannitol. After the mixing for 200 s, the variation of the baseline of the original spectra converged. Also, the variation of second derivative of 1392, 1495, and 1580 nm converged.

Figure 13 shows a plot of a 5-point moving block standard deviation of peak intensities at 1392, 1495, and 1580 nm in the second-derivative spectra versus time. During the initial stage of mixing, the power sample in the bottle is inhomogeneous, and therefore, the spectra, in which bands mainly due to either D-mannitol or talc are dominant, are detected at every measurement, causing a high standard deviation value. As mixing proceeds, the sample becomes homogeneous; then, the spectra of the mixtures of D-mannitol and talc as the mixing ratio are detected, and thus, the spectral variation decreases, yielding a low standard deviation value. The results shown in Fig. 13 show that the standard deviation gives a constant value of 200 s after the start of rotation mixing. Thus, it is very likely that the sample in the bottle becomes homogeneous after 200 s. The sample homogeneity was confirmed by an existing method carried out for a sample taken from a bottle by offline measurement, and it is found that the developed P-NIRs enables in-line monitoring of mixing samples. These results demonstrate that this P-NIRs has high speed and

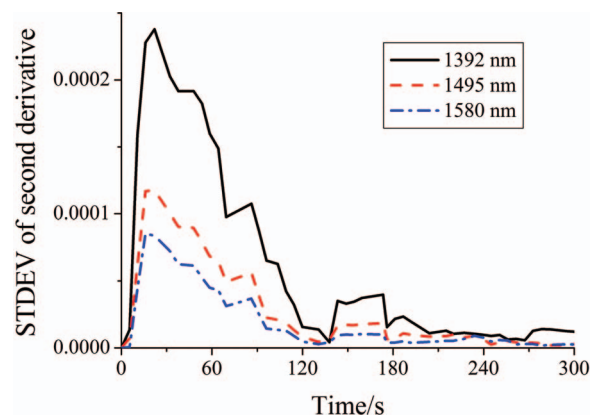


FIG. 13. Plots for standard deviation of the second-derivative absorbance at 1392, 1495, and 1580 nm versus time.

sufficiently compact for realizing in-line monitoring in pharmaceutical processes.

## VI. CONCLUSION

We have developed one of the world's highest density and high-sensitivity array detector to realize a compact, high-resolution, high-sensitivity, and high-speed polychromator-type NIR spectrometer. The P-NIRs shows improved wavelength resolution and high sensitivity by the use of the newly developed PDA detector with 640 elements. Existing NIR spectrometers have PDA detector with at most 512 elements, and thus their wavelength resolution is at best 1.56 nm. However, the developed novel PDA detector has allowed one to reach wavelength resolution of 1.25 nm or even better. Moreover, the combined use of the PDA detector with the developed charge-amplifier array has shortened the measurement time from ca. 3 s to below 10 ms.

Through a mechanical investigation and prototyping of a remote DR detection mechanism required for in-line monitoring of the pharmaceutical process, introduction of high-speed data processing, and addition of functions such as a wireless interface, we have developed a prototype model of a high-speed spectrometer for in-line use and confirmed its performance. In PAT, where one must monitor timely quality parameters and functional properties of pharmaceuticals during their manufacturing process, P-NIRs having high speed is a very suitable NIR spectrometer. Moreover, because of its small size, it is very easy to set it up at various pharmaceutical process lines. We have confirmed that P-NIRs have achieved high speed, high sensitivity, and high resolution by measuring the DR-NIR spectra of D-mannitol and talc in the powder state. Moreover, we have shown that P-NIRs can be used to evaluate the homogeneity of the mixed powder samples through the in-line monitoring of the mixed states of the powder samples.

## ACKNOWLEDGMENTS

The study was financially supported by the Innovation Promotion Program from the New Energy and Industrial Technology Development Organization (NEDO), Ministry of Economy, Trade and Industry, Japan.

- <sup>1</sup>U.S. Food and Drug Administration, *Guidance for Industry, PAT: A Framework for Innovative Pharmaceutical Development, Manufacturing, and Quality Assurance* (U.S. Food and Drug Administration, Maryland, 2004).
- <sup>2</sup>K. A. Bakeev, *Process Analytical Technology* (Blackwell, Oxford, 2005), pp. 13–38.
- <sup>3</sup>Y. Ozaki and T. Amari, *Near-Infrared Spectroscopy in Chemical Process Analysis* (Sheffield Academic, Sheffield, 2000), pp. 53–95.
- <sup>4</sup>T. L. Threlfall and J. M. Chalmers, *Handbook of Vibrational Spectroscopy* (Wiley, New York, 2002), Vol. 5, pp. 423–435.
- <sup>5</sup>U. Hoffmann and N. Zanier-Szydłowski, *J. Near Infrared Spectrosc.* **7**, 33 (1999).
- <sup>6</sup>Y. Wu, Y. Jin, Y. Li, D. Sun, X. Liu, and Y. Chen, *Vib. Spectrosc.* **58**, 109 (2012).
- <sup>7</sup>Y. Ozaki and S. Morita, *Encyclopedia of Applied Spectroscopy* (Wiley, Weinheim, 2009), pp. 872–886.
- <sup>8</sup>F. A. DeThomas and P. J. Brimmer, *Handbook of Vibrational Spectroscopy* (Wiley, New York, 2002), Vol. 1, pp. 383–392.
- <sup>9</sup>E. W. Stark, *Handbook of Vibrational Spectroscopy* (Wiley, New York, 2002), Vol. 1, pp. 393–417.
- <sup>10</sup>Y. Ozaki, *Anal. Sci.* **28**, 545 (2012).
- <sup>11</sup>K. Sakakibara, Y. Sanpei, and A. Miura, Japan patent 4,165,785 (8 August 2008).
- <sup>12</sup>M. Wada and K. Sakakibara, Japan patent Kokai 2002–319696 (31 October 2002).
- <sup>13</sup>M. Komiya, Y. Sanpei, A. Miura, K. Sakakibara, T. Yakhara, T. Fujita, S. Kobayashi, S. Oka, and Y. Akasaka, U.S. patent 6,552,325 B1 (22 April 2003).
- <sup>14</sup>A. Savitky and M. J. E. Golay, *Anal. Chem.* **36**, 1627 (1964).
- <sup>15</sup>S. S. Sekulic, H. W. Ward II, D. R. Brannegan, E. D. Stanley, C. L. Evans, S. T. Sciavolino, P. A. Hailey, and P. K. Aldridge, *Anal. Chem.* **68**, 509 (1996).
- <sup>16</sup>O. Berntsson, L.-G. Danielsson, B. Lagerholm, and S. Folestad, *Powder Technol.* **123**, 185 (2002).
- <sup>17</sup>Y. Roggo, P. Chalut, L. Maurer, C. Lema-Martinez, A. Edmond, and N. Jent, *J. Pharm. Biomed. Anal.* **44**, 683 (2007).
- <sup>18</sup>S. Petit, A. Decarreau, F. Martin, and R. Buchet, *Phys. Chem. Miner.* **31**, 585 (2004).